

Oxyanion Adsorptions by Mono-, Di-, and Triamino-Functionalized MCM-48

Hideaki Yoshitake,* Toshiyuki Yokoi,[†] and Takashi Tatsumi[†]

Graduate School of Environment and Information Sciences, Yokohama National University,
79-7 Tokiwadai, Hodogaya-ku, Yokohama 240-8501

[†]Division of Material Sciences, Graduate School of Engineering, Yokohama National University,
79-5 Tokiwadai, Hodogaya-ku, Yokohama 240-8501

(Received August 14, 2002)

MCM-48 is functionalized with mono-, di-, and triamino-silanes without destruction of the mesoporous structure in order to efficiently remove chromate and arsenate in aqueous solutions. The adsorption capacities achieved 160 and 182 mg/g-adsorbent for chromate and arsenate, respectively, when triamino-functionalized MCM-48 was applied. The diamino-functionalized MCM-48 adsorbed much larger amounts of chromate and arsenate: 119 and 122 mg/g-adsorbent, respectively, than did diamino-functionalized fumed silica: 79.3 and 90.7 mg/g-adsorbent. The superiority arose from the large surface area of functionalized MCM-48. At the adsorption saturation, no clear difference was found in oxyanion/N stoichiometries among the mono-, di-, and triamino-functionalized MCM-48. On the other hand, the distribution coefficient, K_d , depended on the kind of silane fixed on MCM-48. It exceeded 2×10^5 when the concentration of oxyanions was low. The adsorbent by triamino-silylation showed the largest K_d ; it was three or ten times higher than that of the adsorbent by monoamino-silylation for arsenate and chromate adsorptions, respectively. Although the adsorption capacity of diamino-functionalized MCM-48 was reduced to be 47% at 50 °C, it still adsorbed a large amount of arsenate.

The exposure to toxic oxyanions such as arsenate and chromate in groundwater is a rising environmental problem. The chronic toxicity of arsenate has been reported as causing the emergence of blackfoot disease in Taiwan^{1,2} and of various cancers in Bangladesh.³ Chromium has been used in electroplating and tanning industries and untreated effluents from such industries pollute the groundwater.^{4,5} A simple solution is necessary for the water supply in well-dependent societies. Adsorption on solid surfaces is considered to be an effective method. The adsorption uptakes of arsenates have been investigated for metal-impregnated activated carbon,^{6–8} coral limestone,⁹ lanthanum compounds,¹⁰ iron(III) (hydr)oxides,^{11–14} iron,¹⁵ active alumina,¹⁶ clays,¹⁷ various biological products,^{18–21} bentonite,²² and biomass.^{23–25} Conventional porous solids, such as coconut coir,²⁶ zeolite,^{27–29} and clay minerals,³⁰ modified with amines have been applied to the removal of chromate and arsenate. These composite materials have not always shown successful results. The required properties of the ideal adsorbent are uniformly accessible pores, high density of adsorption sites and environmental adaptability.

The mesoporous molecular sieves synthesized with the aid of micelle templates^{31–34} have shown huge surface areas, well ordered periodic structures, and controllable pore size by varying the template molecule and/or using additives such as trimethylbenzene.^{35,36} These characteristics of mesoporous molecular sieves are attractive in seeking the adsorbents working in the environment. Since the specific adsorption of oxyanions is not expected on silica surfaces, the surface must be functionalized to achieve a meaningful absorption capacity. The adsorption of toxic cations has been already explored for functional groups

fixed on mesoporous silicas. The divalent cations, Cu^{2+} , Zn^{2+} , Cr^{2+} , and Ni^{2+} , are adsorbed on amino-functionalized SBA-15 while Hg^{2+} is preferably adsorbed on thiol-functionalized SBA-15.³⁷ The mercury adsorption on the thiol-functionalized mesoporous silicas has been intensively studied.^{38–41}

Unlike cation adsorptions, the studies on anion removal by functionalized mesoporous silicas are relatively rare. We have demonstrated that the amino-functionalized SBA-1 exhibited a marked capacity for arsenate and chromate adsorptions in acidic conditions.⁴² One oxyanion adsorbed on every two amine sites in mono-, di-, and triamino-functionalized SBA-1. Cu^{2+} -activated diamino-functionalized MCM-41⁴³ also adsorbed chromate and arsenate as much as the number of Cu ions fixed on the surface.

The studies on the adsorption by functionalized mesoporous silicas have stressed the high surface area and the pointed out that mesopores must be large enough to accommodate both functional groups and hydrated ions. Although the results have achieved marvellous adsorption capacities, the influences of the specific mesostructure or the microscopic differences of the adsorption sites are still unclear. One should compare silica materials as well as functional groups in a series for the clarification of the characteristics of structure of mesoframework and adsorption sites on the pores. In this study, adsorptions of arsenate and chromate on protonated amino groups fixed on MCM-48 were investigated as well as the functionalized fumed silica with respect to the adsorption capacity of toxic anion adsorptions. Unlike MCM-41, a monocrySTALLINE particle of MCM-48 has two crossing channels, which allow rapid diffusion of the ions and molecules accommodated in the pores even in the presence of a barrier by blockage of the adsorbates or by partial destruction of

the pore structure. We also explored the differences in adsorption characteristics arising from the variation of mono-, di-, and triamino-silylation of MCM-48. We intended to explore the adsorption modes dependence on the fraction of sites covered by the oxyanions and to offer insights into the effective adsorbents of oxyanions.

Experimental

Mesoporous silicas were synthesized with tetraethyl orthosilicate (TEOS, Tokyo Kasei Kogyo Co., Ltd., reagent grade) as a silica source. Cetyltrimethylammonium chloride (CTMACl, > 98%) and Cetyltrimethylammonium hydroxide (CTMAOH, reagent grade) were available at Tokyo Kasei Kogyo Co., Ltd. 3-Aminopropyltrimethoxysilane ($\text{H}_2\text{NCH}_2\text{CH}_2\text{CH}_2\text{Si}(\text{OCH}_3)_3$) and [3-(2-aminoethylamino)propyl]trimethoxysilane ($\text{H}_2\text{NCH}_2\text{CH}_2\text{NHCH}_2\text{CH}_2\text{CH}_2\text{Si}(\text{OCH}_3)_3$) were also purchased from Tokyo Kasei Kogyo Co., Ltd. Their purities were > 98 and > 95%, respectively. *N*-[3-(trimethoxysilyl)propyl]diethylenetriamine ($\text{H}_2\text{NCH}_2\text{CH}_2\text{HNCH}_2\text{CH}_2\text{NHCH}_2\text{CH}_2\text{CH}_2\text{Si}(\text{OCH}_3)_3$) was obtained from Aldrich. Potassium chromate (K_2CrO_4 , > 99%) and potassium arsenate (KH_2AsO_4 , Pr.G.) were the products of Wako Pure Chemical Industries Ltd.

MCM-48 mesoporous silica was synthesized with tetraethyl orthosilicate (TEOS) as a silica source. TEOS, CTMACl, and CTMAOH were mixed in water and the solution was stirred for 1 h at room temperature. The composition of the gel mixture was Si:CTMACl:CTMAOH: H_2O = 1:0.7:0.3:46.5. The solution was transferred to a Teflon bottle and placed in a 373 K oven for 10 d. White precipitates were filtered, washed with ethanol and dried at 373 K. This as-synthesized powder was calcined at 813 K for 6 h and stored in a desiccator.

The calcined MCM-48 was dehydrated at 423 K in vacuum to remove water molecules adsorbed on the surface and stirred vigorously in toluene containing one monolayer equivalent amount (1.0 per 1 nm^2) of 3-aminopropyltrimethoxysilane, [3-(2-aminoethylamino)propyl]trimethoxysilane or *N*-[3-(trimethoxysilyl)propyl]diethylenetriamine. These solutions were heated to 383 K in dry nitrogen for 6 h. The powder was collected by filtration, washed with 2-propanol for 2 h and dried at 373 K. Then, 100 mg of the powder was stirred in 100 mL of 0.1 M-HCl for 6 h without heating. These mono-, di- and triamino-functionalized silica chlorides are denoted by N-, NN- and NNN-MCM-48, respectively. Cab-O-Sil M5 (Cabot, $S_{\text{BET}} = 170.0 \text{ m}^2/\text{g}$, and $V_p = 39.1 \text{ mm}^3/\text{g}$) was functionalized by the same procedure.

The mesostructural order of all powders was checked by X-ray diffraction (XRD, XL Labo, MAC Science Co., Ltd.) with $\text{Cu K}\alpha$ radiation in 40 kV and 20 mA. Nitrogen adsorption-desorption isotherms were recorded by BELSORP 28SA (BEL Japan Inc.) after the sample was evacuated at 473 K for 2 h.

The standard procedure of adsorption experiments was as follows. 50 mg quantity of modified silica was stirred for 10 h in 100 mL of aqueous solution of KH_2AsO_4 or K_2CrO_4 . The concentration in the solution became constant within 5 h. The solution was filtered to remove the solids and then analyzed by ICP-AES. The detection limit was 1 ppb. Typical pH value of the arsenate solution at the beginning was 6.5; after the adsorption, it decreased by ca. 3. The initial and final pH values of the chromate solutions were typically 8.3 and 4.3. In these pH conditions, the dominant arsenate species in the aqueous solution at the equilibrium is H_2AsO_4^- and HCrO_4^- since the dissociation constants of H_3AsO_4 are $\text{p}K_{a1} = 2.19$, $\text{p}K_{a2} = 6.94$, and $\text{p}K_{a3} = 11.5$ and those of H_2CrO_4 are $\text{p}K_{a1} = -0.7$ and

$$\text{p}K_{a2} = 6.52.^{34,35}$$

Results and Discussion

Figure 1 shows the X-ray diffraction patterns of MCM-48 before and after functionalization with [3-(2-aminoethylamino)propyl]trimethoxysilane. A dominant (211) peak at 2.49° with a small (220) reflection and unresolved (321), (400), (420), (332), (422), and (431) reflections are attributed to those of a cubic (*Ia3d*) structure³⁴ with $a_0 = 8.70 \text{ nm}$. Diaminosilane grafting to MCM-41 caused a decrease in the intensity of higher indices, implying a partial loss of the space correlation of the pores, which has been often observed in the silylation of mesoporous silicas.^{39,44,45} Although the peaks again decreased after protonation, the characteristic reflections are still observable. The pattern clearly shows that mesostructure of MCM-48 remains in protonated NN-MCM-48.

The nitrogen adsorption showed the type IV appearance of the isotherms for MCM-48, NN-MCM-48 and protonated NN-MCM-48. The features are indicative of the presence of well-defined mesopores. The specific surface area (S_{BET}), total pore volume (V_p), and most probable pore size ($2R_p$) in BJH distributions are summarized in Table 1 with the results of elemental analysis, the N content (in mmol per g-powder), and the surface density of N. Upon grafting aminosilanes to the framework walls, the decreases in the surface area, pore volume, and pore size were observed while successive H^+ treatment did not significantly influence upon these parameters. The acid treatment causes the decrease of the surface area in the M41S mesoporous silicas and the grafting of hydrophobic functional groups evades such structural deterioration.⁴⁶ The organic groups inhibiting protons and water molecules from accessing the silica

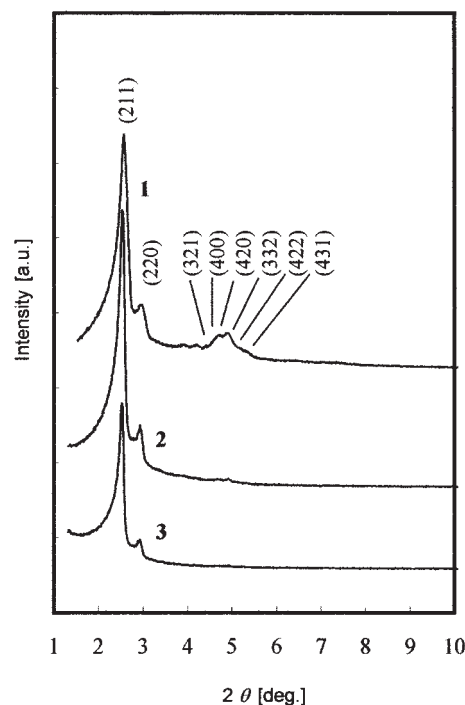


Fig. 1. X-ray diffraction patterns of MCM-48 mesoporous silicas prior to (1) and following (2) functionalization with [3-(2-aminoethylamino)propyl]trimethoxysilane, and after treatment in hydrochloric acid (3).

Table 1. BET Surface Area, Total Pore Volume, Pore Size, Loading of N and Surface Density of N of Functionalized MCM-48

	S_{BET} m ² /g	V_{p} mm ³ /g	$2R_{\text{p}}$ nm	N content mmol/g	N density nm ⁻²
MCM-48	1178	270	3.34	—	—
N-MCM-48	1138	262	3.28	1.53	0.81
H/N-MCM-48	1104	254	3.12	1.37	0.75
NN-MCM-48	894	205	2.70	2.71	1.83
H/NN-MCM-48	898	206	2.73	2.28	1.53
NNN-MCM-48	725	170	2.68	4.15	3.45
H/NNN-MCM-48	640	148	2.56	3.51	3.30
H/NN-Cab-O-Sil	117	26.8		1.43	7.36

surface likely result in “clean protonations” of amino groups without decrease in the surface area. On the other hand, the decrease in S_{BET} , V_{p} , and $2R_{\text{p}}$ clearly depends on the number of amino groups in a silane molecule. This tendency has been observed in the grafting of MCM-41 and SBA-1⁴⁷ while the deterioration of the structure is less grave in MCM-48. For example, 19, 54, and 63% of S_{BET} were lost by N-, NN-, and NNN-functionalization of MCM-41 while the loss of the surface area reached 3, 24 and 38% by the respective treatments of MCM-48 (Table 1). These differences likely arise from the microscopic structure of Si–O–Si bond and/or Si–OH rather than from a mesoscopic feature such as channel connection or curvature of the pore wall. The decrease in the pore size is dependent on the size of the silanes and this finding is consistent with the attribution of the pore tightening to the high density of organic groups on the pore walls.^{39,40,48} The loss of BET surface area by diamino-functionalization of Cab–O–sil is 31%, which is larger than that in MCM-48.

The surface density of amino groups calculated from the results of the elemental analysis (Table 1) demonstrates that the population of functional groups on the adsorbent surface is 0.75–1.1 per nm². In contrast, a dense grafting is realized with Cab–O–sil where the population of en group is 3.7 per nm². This is attributable to the high density of silanols on Cab–O–sil. However, the density of amino group per g-powder (1.43 mmol) is still lower than that of MCM-48 (2.28) due to its low surface area.

Figure 2 shows the infrared spectra of MCM-48 prior to and following grafting by [3-(2-aminoethylamino)propyl]trimethoxysilane. A sharp absorption is observed at 3744 cm⁻¹, while several silanol bands around 3459 cm⁻¹ are not well resolved. The former band has been assigned to isolated Si–OH and the others resulted from the sums of contributions of hydrogen-bonded silanols.^{25,49} Bands at 2931, 2860, 1668, 1606, 1452, and 1351 cm⁻¹ appear at the expense of the band at 3744 cm⁻¹ after silylation; these are assigned to C–H asymmetric stretching, C–H symmetric stretching, two kinds of NH₂ scissor, CH₂ scissor, and CH₃ bending vibrations, respectively. The band positions are similar to those reported in the previous studies.^{47,50} The similar position of the bands appearing at 1300–1700 cm⁻¹ region and a splitting feature of the band for NH₂ scissors suggest that a similar structure of the functional group was likely to be formed on MCM-48. The weak absorption at 1351 cm⁻¹ due to CH₃ bending mode suggests a trace amount of remaining –OCH₃.

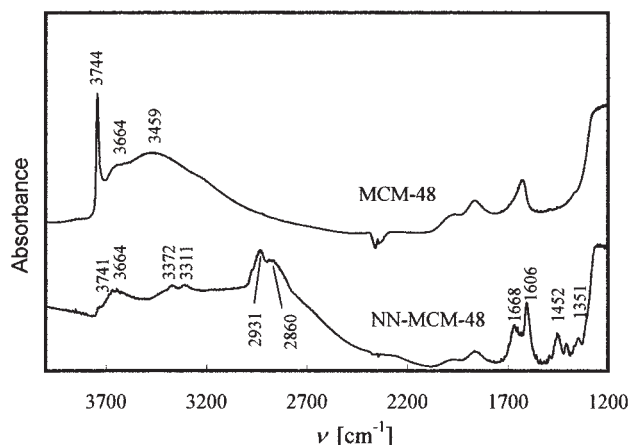


Fig. 2. Infrared spectra of MCM-48 prior to and following functionalization with [3-(2-aminoethylamino)propyl]tri-methoxysilane.

Figure 3 shows the adsorption isotherms of chromate and arsenate on the amino-functionalized MCM-48. The slopes of the initial curves are very steep for both oxyanions until saturation. The initial slope is not significantly dependent on the functional groups. The saturation of these oxyanions increases with increasing the number of nitrogens in the parent silanes, which roughly corresponds to the number of amino groups in the adsorbent powder. However, the maximum adsorption is not proportional to the number of N.

The adsorption capacities are summarized in Table 2 with the stoichiometry of oxyanion to nitrogen. In chromate adsorption, the three kinds of functionalized MCM-48 show slightly smaller Cr/N ratios (0.39–0.45) than NN–Cab–O–sil does (0.48). No significant differences in As/N are found between N-, NN-, and NNN-MCM-48 (0.37–0.38) but these values are slightly smaller than that in NN–Cab–O–sil (0.45). NN–Cab–O–sil, which naturally has little pores, nearly achieves 2 amino-groups-to-1 anion stoichiometry. The average distance between the silanes fixed on the surface is estimated to be $(1/0.75)^{1/2} = 1.2$ nm; the Si–N distance in all trans conformation is ca. 0.5 nm. This reveals that the one anion cannot be coordinated with two amino-groups in a uniform way. In addition, each functional group in NN-MCM-48 completes 2-1 coordination and, consequently, a large difference would appear in anion/N ratio from those for N- and NNN-MCM-48. On the contrary, the ratios are nearly the same in Table 2. These disagreements between the surface density of amino-groups and oxyanion/N stoichiometries imply the heterogeneous distributions of functional groups. The finding that NNN-MCM-48 shows smaller Cr/N ratio than N-MCM-48 does suggests that the distance of the neighbouring organic chains is not crucial in the decrease of the stoichiometry. On the contrary, it is more likely that the “overcrowded” functional groups in the pores suppress this ratio.

In spite of the large anion/N ratio, the adsorption capacity per g-adsorbent of NN–Cab–O–sil does not reach those of NN-MCM-48. This is simply due to the small surface area. The adsorption capacities of NNN-MCM-48, 160, and 182 mg/g-adsorbent for chromate and arsenate, respectively, are outstanding values among the oxyanion adsorbents in the literature. The capacities of chromate adsorption on surfactant modified clay³⁰ and arsenate

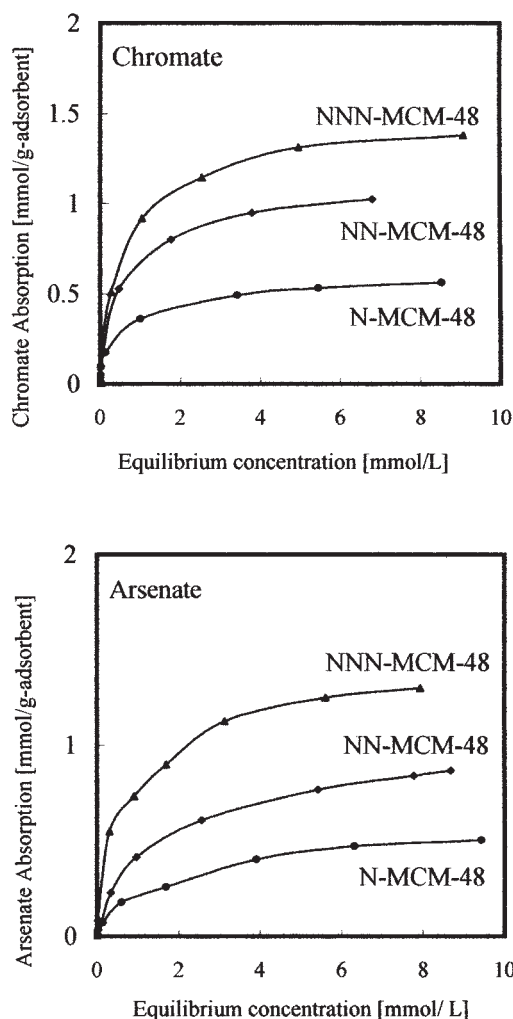


Fig. 3. Adsorption isotherms of chromate and arsenate. 50 mg of protonated functionalized MCM-48 were stirred for 10 h in 100 mL of aqueous solutions of arsenate or chromate at room temperature.

Table 2. Molar Ratio of Anion/N and Specific Adsorption at Saturation

	CrO_4^{2-}		HAsO_4^{2-}	
	Cr/N	mg/g-ads.	As/N	mg/g-ads.
N-MCM-48	0.41	65.4	0.37	70.5
NN-MCM-48	0.45	119	0.38	122
NNN-MCM-48	0.39	160	0.37	182
NN-Cab-O-Sil	0.48	79.3	0.45	90.7

adsorption on activated alumina¹⁶ have been reported to be 40.5 mg/g-adsorbent and 9.93–15.9 mg/g-adsorbent, respectively, which are much smaller than the present result.

The complete removal of these oxyanions, with less than 1 ppb remaining in the solution, is expected for the adsorbents using in the environment. The distribution coefficients, K_d , are thus an important parameter; they are plotted against the fraction of sites covered by oxyanions in Fig. 4. In the small (< 0.1) fraction of sites covered by chromate and arsenate anions, we observed $K_d > 2 \times 10^5$ for the adsorption on NN- and NNN-MCM-48. The

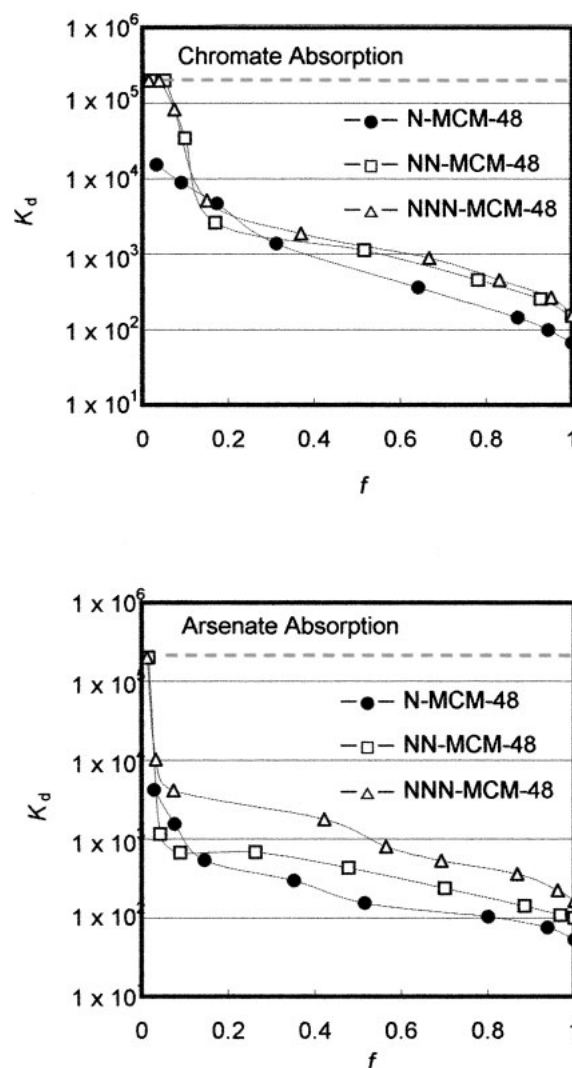


Fig. 4. Distribution coefficient versus fraction of sites covered by adsorbates for protonated N-, NN-, and NNN-MCM-48. Broken lines are the detection limit.

range for chromate where K_d exceeds 2×10^5 is wider than that for arsenate. For both adsorbates, a considerable drop in K_d is found below $f = 0.1$, where f is fraction of sites covered by adsorbate. It decreased to the order of 10^3 and then gradually decreased with f . It is to be noted that K_d still remains around 100 near the saturation (~ 1.0), revealing the excellent performance of these adsorbents. Over most of the f range, triamino-functionalized MCM-48 shows K_d values three or ten times larger than that of monoamino-functionalized MCM-48 in chromate or arsenate adsorptions, respectively. In addition, the maximum K_d we observed for N-MCM-41 is around 1×10^5 . These results demonstrate that the number of amino groups in the organic chain is crucial to K_d , unlike the Cr/N and As/N stoichiometries at the adsorption saturation.

In the Langmuir equation, the equilibrium constant b is presented by $1/f = 1/(bC) + 1$, where C is equilibrium concentration of anions. The fraction of sites covered by adsorbate is proportional to the amount of adsorption, C_m . C_m^{-1} is plotted against C^{-1} in Fig. 5. In all adsorbents, no linearity was found; the slopes were gradually decreased with increase of $1/C$. This

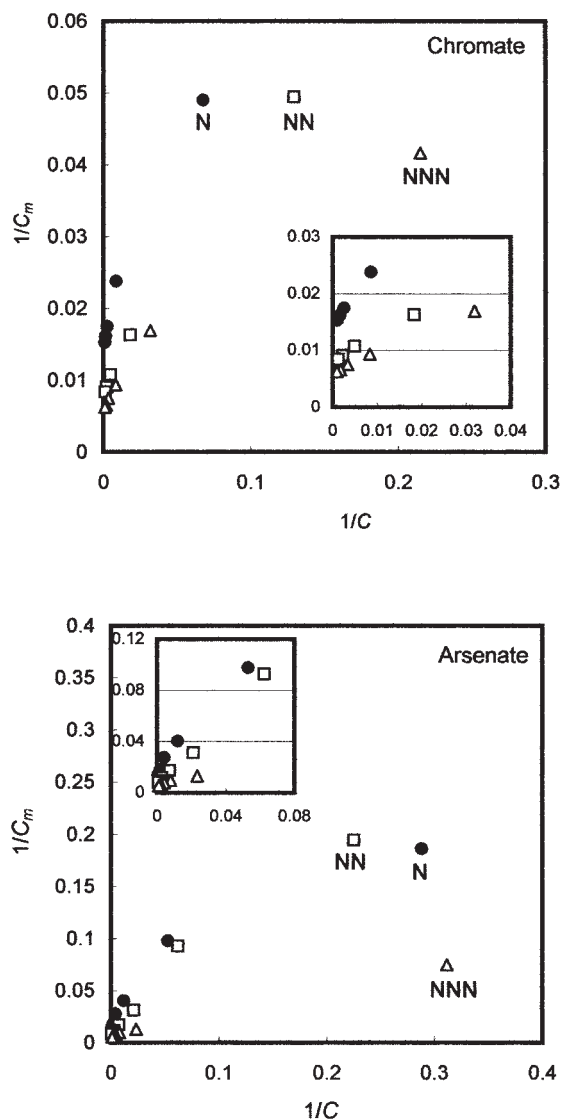


Fig. 5. Langmuir plots of anion adsorbed (mg/g-adsorbent) against equilibrium concentration (mg/L) of chromate and arsenate for protonated N- (●), NN- (□), and NNN- (△) MCM-48.

implies that b decreases with the fraction of sites covered by adsorbate, suggesting the repulsive interactions between the anion species adsorbed on the site and those in the solution. The values b (in mg/L) calculated from the initial slope and the intercepts of y are 58, 56, and 53 for N-, NN-, and NNN-MCM-48 in chromate adsorptions. This means that little difference is found in the equilibrium constant at $C \rightarrow \infty$. For arsenate adsorption, the equilibrium constants for the adsorbents agree in $b = 36$ at this limit. These results demonstrate that the adsorption-desorption equilibria of oxyanions similarly occur on N-, NN-, and NNN-MCM-48 at the adsorption saturations.

Figure 6 shows the adsorption capacity of NN-MCM-48 in arsenate adsorption. At 4 °C, the capacity increased by 17% while it reduced by 53% at 50 °C. In spite of the large reduction at high temperature, the adsorption capacity of the adsorbent still remains high, suggesting a good applicability to the remediation of the actual environment.

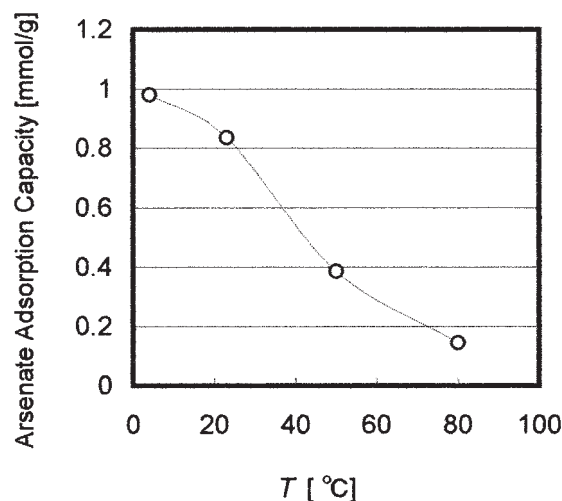


Fig. 6. Adsorption capacity of protonated NN-MCM-48 in various temperatures. 50 mg of protonated functionalized MCM-48 were stirred for 10 h in 100 mL of aqueous solutions of arsenate.

Conclusions

We demonstrated that mono-, di-, and triamino-functionalizations of MCM-48 did not destroy the mesoporous structure and the resultant powder efficiently removed chromate and arsenate in aqueous solutions. The adsorption capacities of triamino-functionalized MCM-48 reached 160 and 182 mg/g-adsorbent for chromate and arsenate, respectively. The capacities of diamino-functionalized MCM-48 (119 and 122 mg/g-adsorbent for chromate and arsenate, respectively) were much larger than those of diamino-functionalized fumed silica, 79.3 and 90.7 mg/g-adsorbent, respectively. This superiority arose from the large surface area of functionalized MCM-48. No clear difference was found in the comparison of oxyanion/N ratio at the adsorption saturation among the mono-, di- and triamino-functionalizations, suggesting that the organic chains are not uniformly distributed on the surface of MCM-48. The distribution coefficient, K_d , for NN- and NNN-MCM-48 exceeded 2×10^5 when the concentration of oxyanions was low. The adsorbent with triamino-silylation showed the largest K_d value; it was three or ten times higher than that with monoamino-silylation for arsenate or chromate adsorptions, respectively. The adsorptions did not follow the Langmuir equation. No significant difference in the equilibrium constant was found among the adsorbents at the adsorption saturations of the oxyanions. Although the adsorption capacity of diamino-functionalized MCM-48 was reduced to be 47% at 50 °C, it still adsorbed a large amount of arsenate, suggesting a good applicability in the environment.

This work was partly supported by Grand-in-Aid for Scientific Research (Grant No. 13780448) from JSPS.

References

- 1 Y. S. Sen and C. S. Shen, *J. Water Pollut. Control Fed.*, **36**, 281 (1964).
- 2 S. L. Chen, S. R. Dzeng, M. H. Yang, K. H. Chiu, G. M.

- Shieh, and C. M. Wai, *Environ. Sci. Technol.*, **28**, 877 (1994).
- 3 R. Nickson, J. McArthur, W. Burgess, K. M. Ahmed, P. Ravenscroft, and M. Rahman, *Nature*, **395**, 338 (1998).
 - 4 M. M. Lawrence, *Environ. Sci. Technol.*, **15**, 1482 (1981).
 - 5 E. L. Tavani and C. Volzone, *J. Soc. Leather Technol. Chem.*, **81**, 143 (1997).
 - 6 C. P. Huang and P. L. Fu, *J. Water Pollut. Control Fed.*, **56**, 233 (1984).
 - 7 C. P. Huang and L. M. Vane, *J. Water Pollut. Control Fed.*, **61**, 1596 (1989).
 - 8 L. V. Rajakovic and M. M. Mitovic, *Environ. Pollut.*, **75**, 279 (1992).
 - 9 A. Ohki, K. Nakayachigo, K. Naka, and S. Maeda, *Appl. Organometal. Chem.*, **10**, 747 (1996).
 - 10 S. Tokunaga, S. A. Wasay, and S.-W. Park, *Water Sci. Technol.*, **35**, 71 (1997).
 - 11 Y. Gao and A. Mucci, *Geochim. Cosmochim. Acta*, **65**, 14 (2001).
 - 12 D. G. Lumsdon, J. C. L. Meeussen, E. Paterson, L. M. Garden, and P. Anderson, *Appl. Geochem.*, **16**, 571 (2001).
 - 13 N. Nilsson, P. Persson, L. Lovgren, and S. Sjoberg, *Geochim. Cosmochim. Acta*, **60**, 4385 (1996).
 - 14 J. S. Geelhoed, T. Hiemstra, and W. H. van Riemsdijk, *Geochim. Cosmochim. Acta*, **61**, 2389 (1997).
 - 15 C. Su and R. W. Puls, *Environ. Sci. Technol.*, **35**, 1487 (2001).
 - 16 T. F. Lin and J. K. Wu, *Water Res.*, **35**, 2049 (2001).
 - 17 M. P. Elizalde-Gonzales, J. Mattusch, R. Wennrich, and P. Morgenstern, *Microporous Mesoporous Mater.*, **46**, 277 (2001).
 - 18 J. Chen and S. Yiaccoumi, *Sep. Sci. Technol.*, **32**, 51 (1997).
 - 19 C. M. Elson, D. H. Davies, and E. R. Hayes, *Water Res.*, **14**, 1307 (1980).
 - 20 R. A. A. Muzzarelli, F. Tanfani, and M. Emanuelli, *Carbohydr. Polym.*, **4**, 137 (1984).
 - 21 L. Dambies, E. Guibal, and A. Roze, *Colloids Surf. A*, **170**, 19 (2000).
 - 22 S. A. Khan, R. Rehman, and M. A. Khan, *Waste Manag.*, **15**, 271 (1995).
 - 23 K. S. Low, C. K. Lee, and C. Y. Lee, *Appl. Biochem. Biotechnol.*, **90**, 75 (2001).
 - 24 Y. Nakano, K. Takeshita, and T. Tsutsumi, *Water Res.*, **35**, 496 (2001).
 - 25 S. A. Dean and J. M. Tobin, *Resour. Conserv. Recy.*, **27**, 151 (1999).
 - 26 A. U. Baes, T. Okuda, W. Nishijima, E. Shoto, and M. Okada, *Water Sci. Technol.*, **35**, 89 (1997).
 - 27 G. M. Haggerty and R. S. Bowman, *Environ. Sci. Technol.*, **28**, 452 (1994).
 - 28 Z. Li and R. S. Bowman, *Environ. Sci. Technol.*, **31**, 2407 (1997).
 - 29 Z. Li, *J. Environ. Qual.*, **27**, 240 (1998).
 - 30 B. S. Krishna, D. S. R. Murty, and J. B. S. Prakash, *Appl. Clay Sci.*, **20**, 65 (2001).
 - 31 T. Yanagisawa, T. Shimizu, K. Kuroda, and C. Kato, *Bull. Chem. Soc. Jpn.*, **63**, 988 (1990).
 - 32 S. Inagaki, Y. Fukushima, and K. Kuroda, *J. Chem. Soc., Chem. Commun.*, **1993**, 680.
 - 33 C. T. Kresge, M. E. Leonovicz, W. J. Roth, J. C. Vartuli, and J. S. Beck, *Nature*, **710**, 359 (1992).
 - 34 J. S. Beck, J. C. Vartuli, W. J. Roth, M. E. Leonowicz, C. T. Kresge, K. D. Schmitt, C. T.-W. Chu, D. H. Olson, E. W. Sheppard, S. B. McCullen, J. B. Higgins, and J. L. Schlenker, *J. Am. Chem. Soc.*, **114**, 10834 (1992).
 - 35 J. Y. Ying, C. P. Mehnert, and M. S. Wong, *Angew. Chem., Int. Ed.*, **38**, 56 (1999).
 - 36 A. Corma, *Chem. Rev.*, **97**, 2373 (1997).
 - 37 A. M. Liu, K. Hidajat, S. Kawi, and D. Y. Zhao, *Chem. Commun.*, **2000**, 1145.
 - 38 X. Feng, G. E. Fryxell, L. Q. Wang, A. Y. Kim, J. Liu, and K. M. Kemner, *Science*, **276**, 923 (1997).
 - 39 L. Mercier and T. J. Pinnavaia, *Environ. Sci. Technol.*, **32**, 2749 (1998).
 - 40 J. Brown, R. Richer, and L. Mercier, *Microporous Mesoporous Mater.*, **37**, 41 (2000).
 - 41 R. I. Nooney, M. Kalyanaraman, G. Kennedy, and E. J. Maginn, *Langmuir*, **17**, 528 (2001).
 - 42 H. Yoshitake, T. Yokoi, and T. Tatsumi, *Chem. Lett.*, **2002**, 586.
 - 43 G. E. Fryxell, J. Liu, T. A. Hauser, Z. Nie, K. F. Ferris, S. Mattigod, M. Gong, and R. T. Hallen, *Chem. Mater.*, **11**, 2148 (1999).
 - 44 X. S. Zhao and G. Q. Lu, *J. Phys. Chem. B*, **102**, 1556 (1998).
 - 45 V. Autochshuk and M. Jaroniec, *Chem. Mater.*, **12**, 2496 (2000).
 - 46 K. A. Koyano, T. Tatsumi, Y. Tanaka, and S. Nakata, *J. Phys. Chem., B*, **101**, 9436 (1997).
 - 47 H. Yoshitake, T. Yokoi, and T. Tatsumi, *Chem. Mater.*, **14**, 4603 (2002).
 - 48 W. M. van Rhijn, D. E. de Vos, B. F. Sels, W. D. Bossaert, and P. A. Jacobs, *Chem. Commun.*, **1998**, 317.
 - 49 A. Jentys, N. H. Pham, and H. Vinek, *J. Chem. Soc., Faraday Trans.*, **92**, 3287 (1996).
 - 50 J. F. Diaz and K. J. Balkus, Jr., *Chem. Mater.*, **9**, 61 (1997).